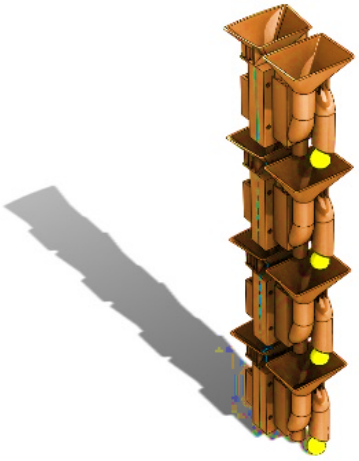

Insights into MFC stacks treating urine; practical challenges for practical implementation

[a]Papaharalabos, G., [b]Greenman, J., [a]Stinchcombe, A., [a]Melhuish, C., & [a*]Ieropoulos, I.

[a]Bristol BioEnergy Centre, Bristol Robotics Laboratory, University of the West of England, Bristol BS16 1QY, United Kingdom

[*]Now at the Civil, Maritime & Environmental Engineering, University of Southampton, SO16 7QF, UK

[b]Faculty of Applied Sciences, University of the West of England, Bristol, United Kingdom

Abstract

Urine is a significant by-product of human metabolism, contributing 75% of nitrogen, 50% of phosphorus, and 10% of the chemical oxygen demand (COD) in municipal wastewater, which can lead to water eutrophication. Microbial Fuel Cells (MFCs) use microorganisms to reduce the organic content in urine while generating electricity and recycling harmful chemicals.

To enhance MFC performance, stacking them in fixed configurations can increase the active surface area for effluent processing. This study assessed a 24-MFC stack fueled by urine under varying hydraulic and electrical conditions to simulate a real-scale MFC scenario for wastewater treatment.

Twenty-eight different electrical and hydraulic configurations showed varying effects on COD removal and power output. The addition of MFC units in a cascade, both in-series and in-parallel, indicated performance trends and identified optimal power-to-COD ratio configurations.

Introduction

MFC stacks: harnessing the power of urine

Urine is an inexhaustible by-product of human metabolism, and on average, healthy individuals produce approximately 2.5 litres of urine *per* day. It is a water-based solution comprising mostly nitrogen (urea), phosphate, potassium, urinary calcium and carbon [1]. On average, urine is responsible for 75% of the nitrogen, 50% of the phosphorous and 10% of the chemical oxygen demand (COD) content found in municipal wastewater, primarily involved in water eutrophication and poisoning of the water horizon [2]. That assumes that if urine is processed separately from municipal waste, it could significantly decrease the need for high-cost segregation and breakdown of chemicals [3]. Because the urine composition also reflects the average requirement of nutrients for plant growth [4], many studies have attempted nutrient removal from urine for industrial usages,

such as ammonia and struvite ($MgNH_4PO_4$) [3,5–11], and their use as fertilisers in agriculture [2,6,11–14]. Many studies in microbial fuel cells (MFCs) have shown that electro-active/anodophillic bacteria can utilise urine as an alternative substrate fuel for direct electricity generation *and resource recovery* [15–22].

MFCs consist of microorganisms capable of reducing the organic content and other compounds found in urine whilst generating reasonable amounts of electricity [23–25] with the added benefit of recycling chemicals harmful to the environment [15]. Elements, such as N, P, K, can be transformed *via* bacterial metabolism into new biomass, thus, removed from the solution, resulting in element reuse. Moreover, the MFC technology features hydrogen generation through urea electrolysis in urine [16].

The ability of MFCs to generate electricity from domestic wastewater [24,26] with the concomitant decrease of organic content has been a semantic area of research due to its advantages over aerobic treatment processes [27]. The bioanodes of MFCs allow for a higher active surface area of microbial communities (biodegradation factor) for processing the effluent as in a trickling filter treatment process (*i.e.* volcanic rocks, lava, coke, gravel). A previous study [28] used a seven-MFC stack to demonstrate a small-scale cascade scenario whereby the power output from each MFC correlates with the availability of organic content (acetate concentration) as it degrades down the effluent stream. This concept has previously been used for oxidising glucose and sucrose solutions [29,30], landfill leachate [31], and human faeces [32] by using relatively large MFC reactors ranging from 0.25 L to 1.5 L. The authors suggested that the higher the effluent's carbon concentration, the less affected the power levels were in the MFCs close to the effluent's exit point.

An effective way to increase the performance of individual MFC units is through the connection of multiple MFCs in stack configurations [33,34] . To date, MFC stacks fuelled by urine have demonstrated the charging of a mobile phone [21,35], and the applicability of the MFC technology in waste recycling and utilisation.

The present study will examine the performance characteristics of a 24-MFC stack supplied with urine under eight hydraulic formations and the corresponding electrical configurations. Each scenario investigates the effect on COD removal and electrical output of the electrical and hydraulic shuffling of MFCs within the stack. The gradual addition of MFC units under the same cascade will reveal performance trends (and operational patterns) related to substrate utilisation downstream, suggesting the optimum Power-to-COD ratio configuration.

Materials & Methods

MFC design

Twenty-four identical open-to-air cathode MFCs[36] operated in different electrical and hydraulic configurations (**Error! Reference source not found.**). Each MFC has an anode volume of 6.25 ml and a projected electrode surface area of 6 cm^2 against the cathode. A catalyst-free carbon fibre veil (Composite Materials, UK) and a single microporous layer (MPL) assembly served as an anode (168 cm^2) and cathode (7 cm^2),

respectively, based on previous work[37]. An ion-exchange membrane (CMI-7000, Membranes International Ltd., USA) separated the anode and the cathode. Titanium wire on both electrodes worked as a current collector (50 mm x 0.5 mm Ø).

MFC stack parameters

MFC reactor design comprises an overflow tube that gravitationally directs the anolyte (i.e. urine) to the MFC underneath it, allowing for stable hydraulic retention time (HRT) and possibly a higher coulombic efficiency [38,39] (**Fig 1A**). MFCs maintained an air gap between sequential units, thus eliminating the substrate cross-conduction effect [40]. A bespoke toggle switch device allowed manual shifting between series to parallel electrical connections of the stacked MFCs [41] (**Fig 1B**). The terms **in-parallel** and **in-series** used in the manuscript describe the **electrical configurations**, whereas the **hydraulic connections** are expressed either with the term **cascaded or staged**.

The experimental setup consists of eight phases whereby the different cascade groups and the electrical configurations start from twenty-four individually fed MFCs, and gradually expand to twenty-four staged MFCs (

Table 1). Throughout the experiments, all the electrical configurations matched the hydraulic setups for maintaining a physical/electrical balance (i.e. subdivisions of twenty-four)

Table 1. Available electrical and hydraulic combinations in the 24 MFC stack

Phase no	Hydraulic connections	Electrical connections			
		Series	Parallel	SxP	PxS
1	1 unit (x24 uni separately fed)	24S	24P	NA*	NA*
2	2 (x 12 groups)	24S	24P	2Sx12P	2Px12S
3	3 (x8)	24S	24P	3Sx8P	3Px8S
4	4 (x6)	24S	24P	4Sx6P	4Px6S
5	6 (x4)	24S	24P	6Sx4P	6Px4S
6	8 (x3)	24S	24P	8Sx3P	8Px3S
7	12 (x2)	24S	24P	12Sx2P	12Px2S
8	24	24S	24P	NA*	NA*

*NA: not applicable

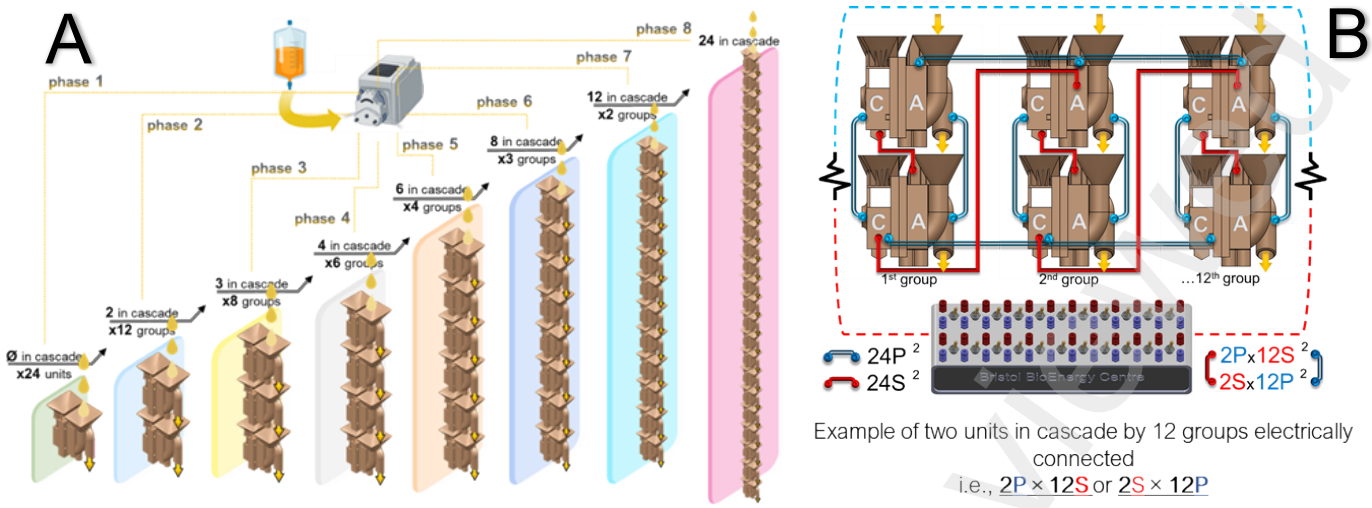

Fig 1. (A) Schematic of the eight hydraulic scenarios and MFC unit repositioning under the same waste stream. (B) Example of a 2unitsx12groups scenario with electrical connections in the stack, denoted by superscript suffixes for hydraulic units in cascade. (C) Lab-scale paradigm of the 24 MFC stack with three electrically connected assemblages, each containing eight MFC units in a hydraulic cascade (8unitsx3groups).

Operational parameters

To inoculate the anodes, the activated sludge waste was used by Wessex Water Scientific Laboratory (Saltford, UK) and was mixed with TYE medium (Tryptone and Yeast Extract; 1% and 0.5%). A 24-channel peristaltic pump (Watson Marlow, UK) maintained a substrate flow rate of 1 mL h^{-1}, corresponding to an HRT of 6.8 hours *per* reactor. All MFCs operated in a batch-fed mode, each connected to a 2.7 kΩ resistor until stable power outputs and no power overshoots [42] were observed. Following the start-up period, the substrate switched to neat human urine. In phase 1, each MFC received substrate from a dedicated twenty-four substrate channel, a single source. After that, the new feedstock channels gradually decreased as more MFCs were supplied in a cascade manner from the preceding unit(s) along the waste stream. At the beginning of each stage and every time that the number of units increased in a cascaded group, the stack was isolated electrically and left in the open-circuit (OCV) state for two hours, with fresh urine being pumped into the system to purge any decomposed residue. Voltages were logged for three hours until the OCV had reached a steady state.

MFCs and overall stack voltage were recorded using an HP Agilent multiplex logging module (34907A, HP). The current was measured in milliamperes (mA) and power in milliwatts (mW). The power produced per unit surface area was calculated by dividing power by the electrode's surface area in square metres (m^2). Voltammetric sweeps of an individual or stacked MFCs were performed by scanning through a range of fifty resistance values from 1 MΩ down to 10 Ω every five minutes, either with the use of a manual or a digitised variable resistor device [43].

Carbon content was measured before and after exiting the MFCs (24-48 h). High-range potassium dichromate oxidation method vials (CAMLAB, UK) were used for colourimetric analysis (Photometer-System MD200, Lovibond) of the chemical oxygen

demand (COD) values. Additionally, urine samples were exposed to air and in air-tight closed bottles on the bench to examine whether atmospheric oxygen affected the oxidation of urine without being processed by MFCs[44]. The pH was measured with a Hanna 8424 pH meter (Hanna, UK) and the conductivity with a 470 Jenway conductivity meter (Camlab, UK). The measured pH of fresh urine samples ranged between 5.5 and 5.8; a conductivity pf ~38 mS from 24 samples and an average COD ranged between 11-16g/L. All experiments were performed under a controlled room temperature of 22 ±1 C.

Results and discussion

Phase 1: Individual units

A performance baseline for the microbial fuel cells (MFCs) was established by testing stacked and standalone units. The average maximum power density (PD) of twenty-four individual MFCs was 6.6 mW/m², and the average current density (CD) was 18 mA/m², with an internal resistance (Rint) of 800 Ω. In the parallel configuration, the stack had an Rint of 22 Ω, yielding a PD of 5 mW/m² and a CD of 22 mA/m². The series connection produced a PD of 5.2 mW/m² and a much lower CD of 1.1 mA/m² due to a higher Rint of 11 kΩ but generated a total current of 438 µA, which was 28% higher than the 314 µA from individual units [45].. Individual MFCs achieved a 19% chemical oxygen demand (COD) removal rate, while series and parallel connections recorded 17% and 23%, respectively, matching findings to previously reported works [46,47].

Phase 2: Two-unit cascade

The first cascade configuration of MFCs in fluidic pairs produced a PD of 7.21 mW/m² and a CD of 29.2 mA/m², improving performance by 30% and 18%, respectively. When adding two electrical parallel and series elements, PD increased by 5% and decreased by 8%. Twelve in series and two in parallel achieved 6.75 mW/m², while twelve in parallel and two in series produced 6.58 mW/m². Adding parallel elements significantly increased CD by 61%, while series elements reduced it by 77%[47]. The performance improvement of this configuration is attributed to the high organic content in urine supporting microbial growth[28]. This, combined with the low retention time, allows for adequate nutritious substrate to reach the nether MFC [31]. Furthermore, previous studies have shown that the metabolic activity of bacteria in the upper MFC provides by-products or shorter chain compounds easily accessible for the lower MFC to process [31,32,48].

Arranging MFCs in parallel achieved a 31% COD removal, 8% higher than single units. Series configuration yielded a 16% COD treatment, a 1% drop from the 17% achieved only in series. Configuring 12 in parallel and 2 in series achieved a COD treatment of 23%, although this indicated a negative impact from the series elements. Conversely, changing to 12 in series and 2 in parallel improved COD treatment to 19%. Despite the enhancements, Rint increased significantly, remaining stable at 21 Ω for parallel connections but reaching 25 kΩ in series. Configuring 12 in parallel and 2 in series brought Rint to 166 Ω, while 12 in series and 2 in parallel lowered it to 2.8 kΩ. This suggests that parallel elements are crucial in managing resistance and maintaining performance efficiency[47].

Phase 3: Three-unit cascade

In the third stage, sequential triplets of MFC units were arranged in 8 hydraulically insulated groups, electrically configurable via a switch box. Testing four configurations revealed that MFCs in parallel achieved a power density (PD) of 3.47 mW/m² and a current density (CD) of 11 mA/m². In series, the PD increased to 4.08 mW/m² but the CD dropped to 0.6 mA/m². A configuration of 8 parallel groups of 3 MFCs in series yielded a PD of 3.57 mW/m² and CD of 5 mA/m², while 8 series-connected groups of 3 in parallel showed a PD of 3.97 mW/m² and CD of 1.9 mA/m².

Despite an initial performance increase with the second unit, adding a third MFC led to decreased overall performance, likely due to the pre-processed substrate negatively impacting the output of subsequent units. This trend was evident across the electrical configurations. Maintaining a consistent flow rate[49], optimised for high COD removal, is suggested to restore power levels.

Following the change in current densities, COD treatment showed a downward trend across configurations. The parallel connection treated 29% (down by 3%), while the series configuration maintained its treatment capacity despite a slight CD decrease (5%). The configurations combining series and parallel chains also exhibited a 3% reduction in COD efficacy.

Internal resistance (Rint) increased in parallel by 70% (to 70 Ω) and decreased in series by 20% (to 20 kΩ). Other configurations displayed a similar negative trend, indicating that reduced carbon energy affected the third MFC's performance.

Parallel MFCs achieved a 31% organic content removal, 8% higher than individual units, while series configurations achieved a 16% COD treatment, a 1% decrease. Other configurations supported better remediation outcomes. However, parallel connections helped manage Rint, keeping it lower in parallel (21 Ω) versus series (25 kΩ), indicating improved efficiency.

Phase 4: Four-unit cascade

Quadruplet MFC units formed six hydraulically insulated groups with a total substrate flow of 6 mL/h. Parallel arrangements achieved a PD of 3.75 mW/m² (3% drop) and a CD of 10.7 mA/m². In series, PD was 2.73 mW/m² (12% drop), and CD was 0.56 mA/m² (18% drop). The other configurations showed significant reductions due to poor feeding conditions for later units.

The in-series configuration resulted in an 18% COD removal; the parallel showed 27%. Rint increased with power loss, doubling to 42 kΩ in series.

Phase 5: Six-unit cascade

Four groups operated at 4 mL/h substrate flow with two additional MFC units. In parallel, PD was 2.05 mW/m² (39% drop), and CD increased slightly to 11 mA/m². The series yielded PD of 1.76 mW/m² (35% drop) and CD of 0.32 mA/m². The mixed configuration produced a PD of 2.22 mW/m² and a CD of 2.34 mA/m², indicating a notable current density increase.

The parallel configuration achieved 33.6% COD removal, the highest in this experiment. The series connection resulted in a 12% COD reduction, and the mixed configuration attained a 30% reduction.

Phase 6: Eight-unit cascade

In Stage 6, adding two units formed groups of 8 MFCs in various electrical configurations. The parallel setup had a power density (PD) of 2.19 mW/m² and a current density (CD) of 8.8 mA/m² at an MPP of 70 Ω, while series configuration yielded a PD of 1.61 mW/m² and a CD of 0.26 mA/m² at 24 kΩ. The mixed configuration (8 in parallel, 3 in series) achieved 2.21 mW/m² and 2.34 mA/m² at 1 kΩ, and the reverse (8 in series, 3 in parallel) provided 1.86 mW/m² and 1.06 mA/m² at 4 kΩ. Power outputs decreased slightly across configurations, with the parallel setup showing a more stable performance.

For COD treatment, the parallel configuration reduced COD by 33.2% after 48 hours, with Rint rising from 40 Ω to 70 Ω. In series, COD reduction was 9%, with Rint up to 60 kΩ. The combination of parallel with series reduced COD by 28%, with Rint at 1 kΩ, while the opposite configuration reduced COD by 15%

Phase 7: Twelve-unit cascade

Stage 7 involved a cascade of 12 units in two rows. Parallel configuration yielded a PD of 2.4 mW/m² and a CD of 10.2 mA/m², marking increases of 9.5% in power and 16% in current. The series configuration provided a 1.7 mW/m² PD and a CD of 0.4 mA/m². Various arrangements further optimised outputs, particularly the parallel with series setup.

In this stage, MFCs were rearranged, moving units away from the feeding source without negatively impacting performance. Regarding COD treatment, the cascades reduced urine's organic content by 26% in parallel and 12% in series, with Rint increasing variably. Thus, if all parameters remained the same, these biofilms would be expected to sustain similar electro-active activity. Furthermore, the biofilms previously deprived of unprocessed urine and now being provided with richer feedstock are likely to recover to a previous state of metabolic activity that allows for a better electrogenic performance [28].

Phase 8: Twenty-four-unit cascade

Stage 8 tested a 24-unit cascade in parallel and series. The parallel configuration achieved a PD of 3.4 mW/m² and a CD of 14.4 mA/m², while the series setup produced lower outputs. Overall, performance improvements were consistent across the phases with various configurations.

COD treatment degraded 22% when configured in parallel and 8% in series, with Rint at 40 Ω and 40 kΩ, respectively. The decrease in COD removal, alongside the increase in current density, indicated efficient substrate conversion to electricity[50], supported by the large number of MFCs in the cascade.

Overview of performance characteristics

A 2-MFC cascade improved the overall power density output compared to individual units. The addition of a third cascade element reduced the overall performance,

and the later introduction of extra units in the same waste stream seemed to decrease the power further, except for the latest stage where the system, configured in parallel electrically, recovered to similar levels as the early stages of the experiment. Nevertheless, as expected, the MFC stack maintained the same decreasing pattern in all electrical configurations and under the different cascade scenarios, with the parallel electrically connected configurations showing the highest average power density generation (Fig.2).

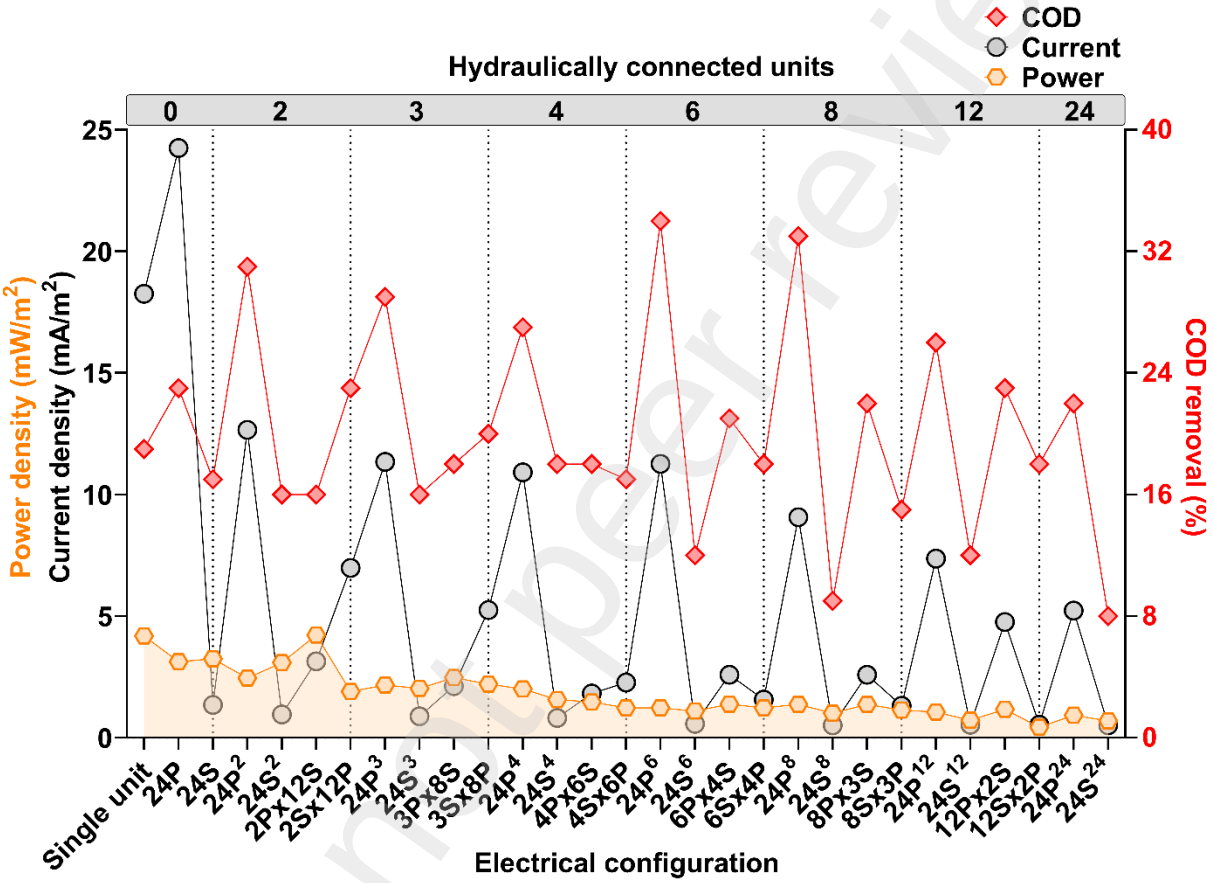

Fig.2 Performance characteristics from all possible cascade and electrical scenarios

Similarly, the increased cascaded units in the stack affected the current generation. This was due to the substrate being utilised in the initial units within the cascade, thus reducing the available organic content down the waste stream, which limited the overall electron extraction(Fig.3). However, the parallel connection improved all the other electrical combinations when comparing the different cascade scenarios. As such, the second-best overall performance in current generation is achieved by introducing parallel elements into the in-series electrically configured stack. This is also highlighted in **Figure 3**, where a constant higher current density is maintained when parallel electrical units are introduced gradually in series connected MFCs and significantly lower current levels when in series electrical elements are brought into an electrically parallel configuration.

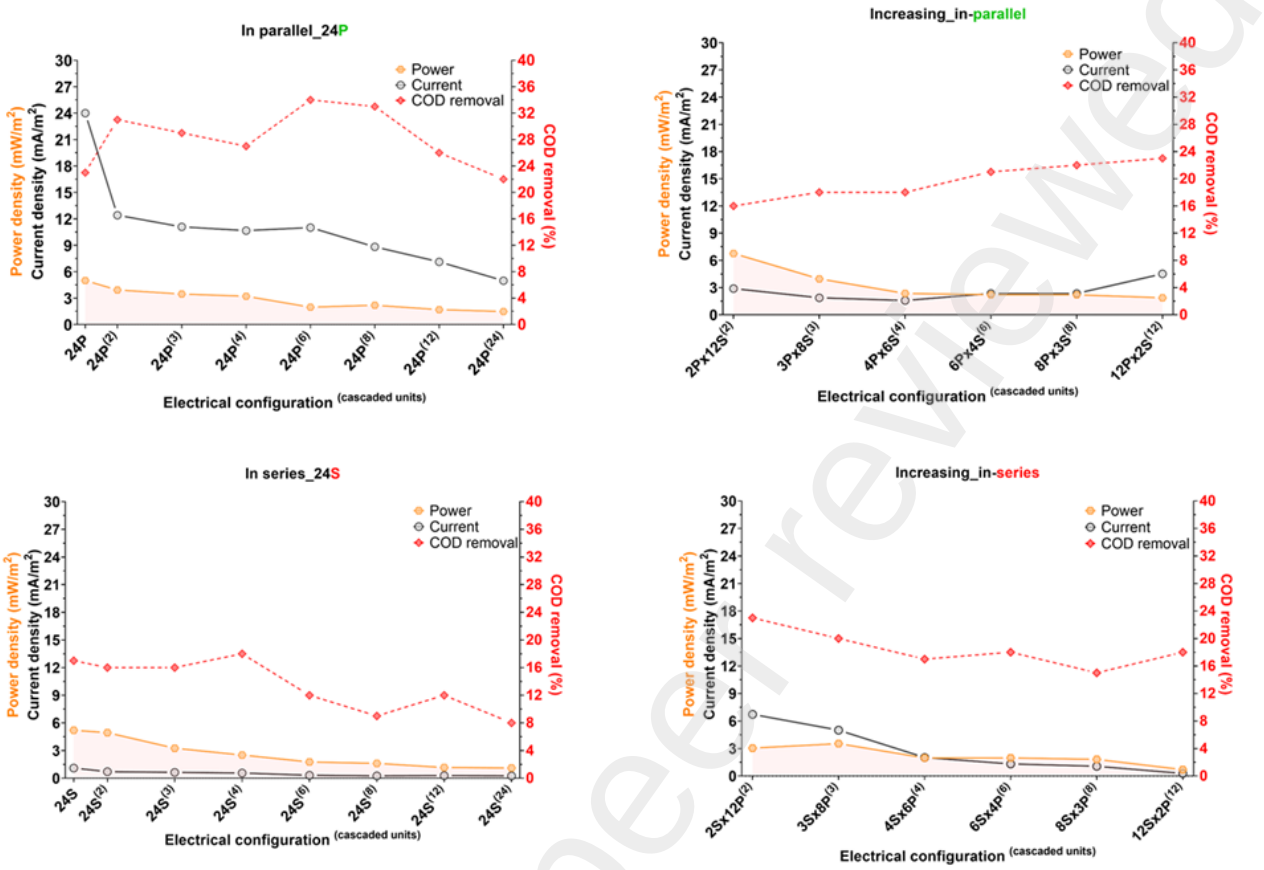

Fig. 3 Breakdown of stack performance behaviour from electrical configuration and cascade scenarios

Overall, the main reasons for this drop in power and current generation could be attributed to (a) the low flow rate that was fixed for the duration of the experiment, (b) the cascade effect, in which the organic load is depleted in the early stages of the cascade; (c) rearranging of robust MFCs from the upper levels of the cascade to the lower levels to increase the MFCs in cascade has possibly resulted in an overall drop in power output.

Adaptation traits of MFC stacks

The experimental data suggested that the shuffling of "healthier" MFCs to lower-quality substrate positions in the cascade positively impacts COD removal when they are connected in parallel rather than in series (**Fig. 4**). Also, reinstating feedstock-deprived MFCs closer to the food source could have an on-off effect on the metabolic activity of their biofilms, where the MFCs recover back to a R_{int} state without necessarily providing the same power and current densities as when they were individually fed.

It is also hypothesised that high numbers of in-series connected MFCs led to a lower performance than parallel connections, possibly derived from polarity reversals within the stack (data not shown). The in-parallel connection created a decreased Rint state within a stack, which allowed for robust operation, negating the appearance of

polarity reversals that can compromise the overall performance and longevity of the system.

The data indicates that COD removal is directly proportional to current generation and inversely proportional to internal resistance (**Fig.5**). Meanwhile, power appears to be a secondary factor in the experimental setup, which maintains a fixed flow rate. However, in a dynamic flow rate scenario, we expect power to increase and have a positive effect on COD removal. Additionally, the results show that the MFC stack can operate effectively even in feedstock-limited situations while maximizing COD removal.

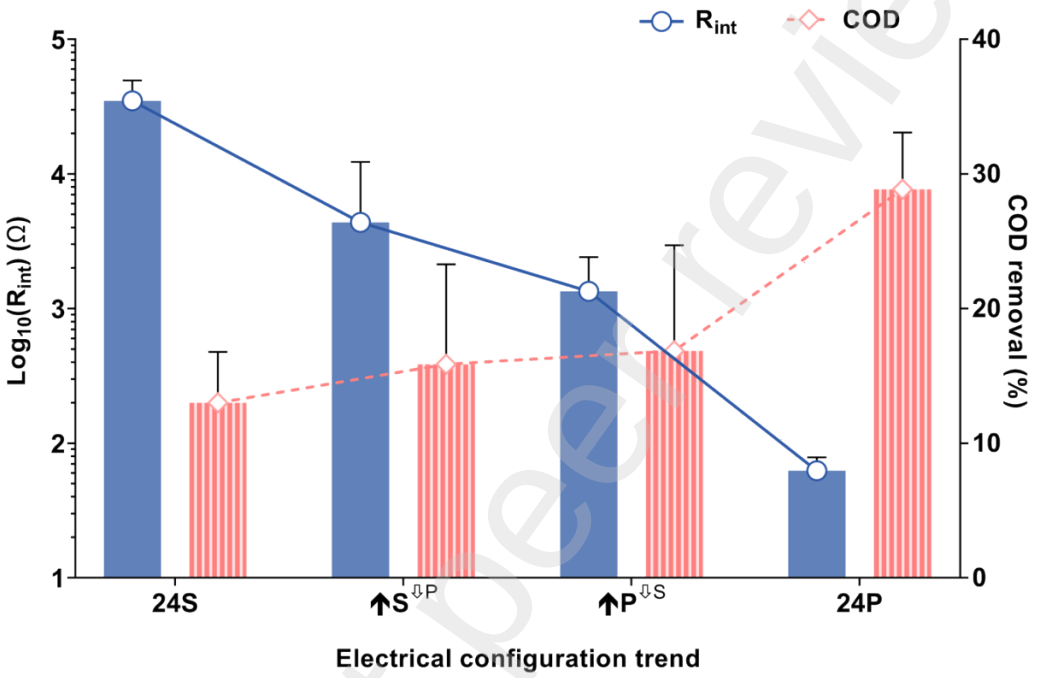

Fig. 4 Trends in internal resistance and COD removal depending on the electrical configuration

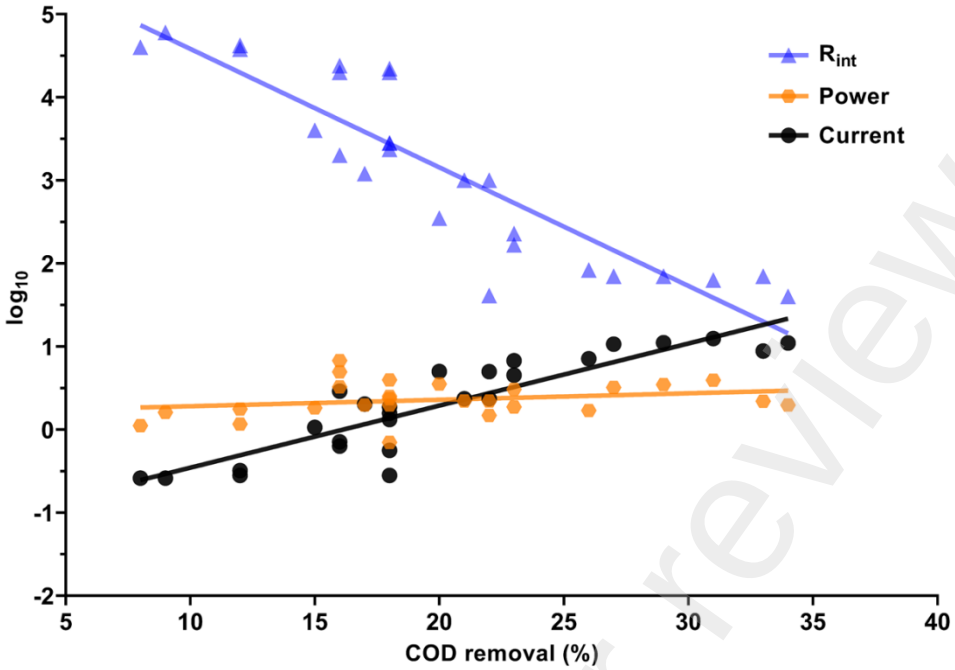

Fig. 5 COD removal correlation between power, current and R_{int}; r_{power} = 0.249 (P = 0.220), $r_{current}$ = 0.891 (P < 0.001), r_{Rint} = -0.891 (P < 0.001)

It is equally important to note that variations in electrical combinations within a cascade can significantly impact current density, Rint, and COD removal. Observations indicate that when parallel elements predominate in the MFC stack, the system exhibits the highest overall power densities, current densities, the lowest internal resistance, and the greatest COD removal rates. Therefore, we can conclude that internal resistance is a key factor influencing the stability and performance of the system. The heatmap in Figure 6 illustrates the optimal hydraulic and electrical combination that ensures resilience and peak operational efficiency.

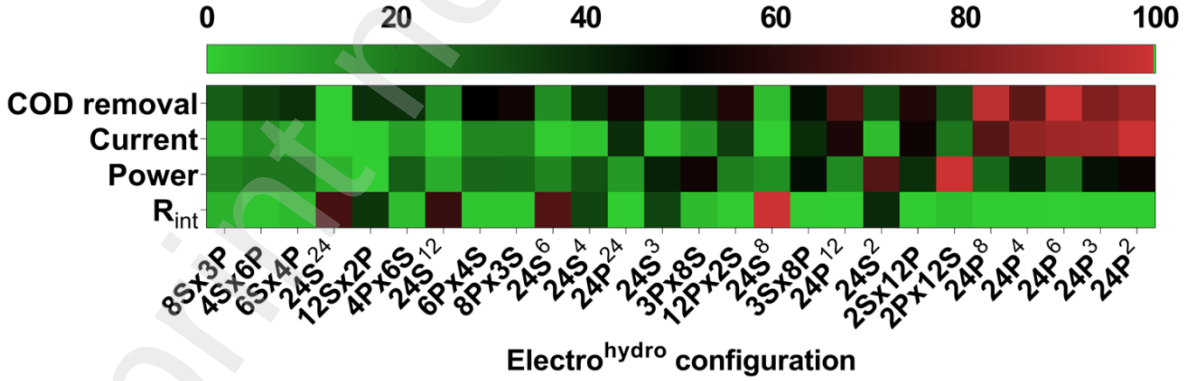

Fig. 6 Heatmap with the optimal electrical and hydraulic combinations

Conclusions

The system must be adaptable when using microbial fuel cells (MFCs) in large-scale wastewater treatment plants. It should be capable of forming different cascaded groups within the waste stream of various sizes, depending on the flow rate and the

required chemical oxygen demand reduction at that stage. Additionally, MFC stacks must adjust their electrical connection configurations based on the dynamic homeostatic status of the biofilms and the power output, ensuring the longevity and smooth operation of the MFC units. This can be achieved by employing a control system that can dynamically reconfigure the stack in real-time, demonstrated previously in a lab environment [51]. This is a critical aspect, which can only be implemented at scale in the real world with further industrial development.

The findings of this study indicate that a cascade configuration is better for wastewater remediation but sacrifices power generation, which decreases due to the limited availability of organic material that reaches the MFCs later in the waste stream. In contrast, a few cascaded units can sustain high power generation levels, especially when configured in a parallel electrical arrangement. It is worth noting that with reference to the data in Fig. 5, an appropriate feedstock supply, adjusted for the number of units/stages in the cascade, would have probably resulted in increasing both power and COD removal; this is a systems engineering challenge that can be addressed with further research and industrial development.

Finally, this study emphasizes the importance of considering urine when designing a large-scale system. Urine exhibits high chemical variability, and many factors can alter its composition, potentially affecting MFC performance and the dominance of specific biofilm species. However, in a theoretical scaled-up system with multiple urinals collecting donations, an MFC stack could serve as a bio-sensing utility, offering valuable information about urine quality based on its power and COD treatment performance.

Acknowledgements

IAI is a Bill & Melinda Gates Foundation grantee and therefore parts of this work have been funded under the grant with no.: INV-042655.

References

1. Rose, C., Parker, A., Jefferson, B. & Cartmell, E. The Characterization of Feces and Urine: A Review of the Literature to Inform Advanced Treatment Technology. *Crit. Rev. Environ. Sci. Technol.* **45**, 1827–1879 (2015).

2. LARSEN, T. & GUJER, W. Separate management of anthropogenic nutrient solutions (human urine). *Water Sci. Technol.* **34**, 87–94 (1996).

3. Larsen, T. A., Maurer, M., Udert, K. M. & Lienert, J. Nutrient cycles and resource management: implications for the choice of wastewater treatment technology. *Water Sci. Technol.* **56**, 229–37 (2007).

4. Heinonen-Tanski, H. & van Wijk-Sijbesma, C. Human excreta for plant production. *Bioresour. Technol.* **96**, 403–11 (2005).

5. Maurer, M., Pronk, W. & Larsen, T. a. Treatment processes for source-separated urine. *Water Res.* **40**, 3151–66 (2006).

6. Liu, Z. *et al.* Urea hydrolysis and recovery of nitrogen and phosphorous as MAP from stale human urine. *J. Environ. Sci. (China)* **20**, 1018–24 (2008).

7. Lienert, J. & Larsen, T. a. Soft paths in wastewater management - The pros and cons of urine source separation. *Gaia* **16**, 280–288 (2007).

8. Udert, K. M., Larsen, T. a., Biebow, M. & Gujer, W. Urea hydrolysis and precipitation dynamics in a urine-collecting system. *Water Res.* **37**, 2571–2582 (2003).

9. Udert, K. M., Larsen, T. a. & Gujer, W. Biologically induced precipitation in urine-collecting systems. *Water Sci. Technol. Water Supply* **3**, 71–78 (2003).

10. Udert, K. M., Larsen, T. A. & Gujer, W. Estimating the precipitation potential in urine-collecting systems. *Water Res.* **37**, 2667–77 (2003).

11. Maurer, M., Schwegler, P. & Larsen, T. A. Nutrients in urine: energetic aspects of removal and recovery. *Water Sci. Technol.* **48**, 37–46 (2003).

12. El Diwani, G., El Rafie, S., El Ibiari, N. N. & El-Aila, H. I. Recovery of ammonia nitrogen from industrial wastewater treatment as struvite slow releasing fertilizer. *Desalination* **214**, 200–214 (2007).

13. Etter, B., Tilley, E., Khadka, R. & Udert, K. M. Low-cost struvite production using source-separated urine in Nepal. *Water Res.* **45**, 852–862 (2011).

14. Ryu, H. D., Lim, C. S., Kang, M. K. & Lee, S. I. Evaluation of struvite obtained from semiconductor wastewater as a fertilizer in cultivating Chinese cabbage. *J. Hazard. Mater.* **221**–**222**, 248–255 (2012).

15. Ieropoulos, I., Greenman, J. & Melhuish, C. Urine utilisation by microbial fuel cells; energy fuel for the future. *Phys. Chem. Chem. Phys.* **14**, 94–8 (2012).

16. Kuntke, P. *et al.* Ammonium recovery and energy production from urine by a microbial fuel cell. *Water Res.* **46**, 2627–36 (2012).

17. Boggs, B. K., King, R. L. & Botte, G. G. Urea electrolysis: direct hydrogen production from urine. *Chem. Commun. (Camb).* 4859–61 (2009). doi:10.1039/b905974a

18. Ieropoulos, I. A., Greenman, J. & Melhuish, C. Miniature microbial fuel cells and stacks for urine utilisation. *Int. J. Hydrogen Energy* **38**, 492–496 (2013).

19. Zang, G.-L. *et al.* Nutrient removal and energy production in a urine treatment process using magnesium ammonium phosphate precipitation and a microbial fuel cell technique. *Phys. Chem. Chem. Phys.* **14**, 1978 (2012).

20. Santoro, C. *et al.* Current generation in membraneless single chamber microbial fuel cells (MFCs) treating urine. *J. Power Sources* **238**, 190–196 (2013).

21. Walter, X. A., Stinchcombe, A., Greenman, J. & Ieropoulos, I. Urine transduction to usable energy: A modular MFC approach for smartphone and remote system

charging. *Appl. Energy* **192**, 575–581 (2016).

22. Walter, X. A. *et al.* Scaling-up of a novel, simplified MFC stack based on a self-stratifying urine column. *Biotechnol. Biofuels* **9**, 93 (2016).

23. Liu, H., Ramnarayanan, R. & Logan, B. E. Production of electricity during wastewater treatment using a single chamber microbial fuel cell. *Environ. Sci. Technol.* **38**, 2281–5 (2004).

24. Habermann, W. & Pommer, E. H. Biological fuel cells with sulphide storage capacity. *Appl. Microbiol. Biotechnol.* **35**, (1991).

25. Logan, B. E. Simultaneous wastewater treatment and biological electricity generation. *Water Sci. Technol.* **52**, 31–7 (2005).

26. Rabaey, K. & Lissens, G. Microbial fuel cells : performances and perspectives. (2005).

27. Kim, B. H., Chang, I. S. & Gadd, G. M. Challenges in microbial fuel cell development and operation. *Appl. Microbiol. Biotechnol.* **76**, 485–94 (2007).

28. Winfield, J., Ieropoulos, I. & Greenman, J. Investigating a cascade of seven hydraulically connected microbial fuel cells. *Bioresour. Technol.* **110**, 245–50 (2012).

29. Chung, K. & Okabe, S. Continuous power generation and microbial community structure of the anode biofilms in a three-stage microbial fuel cell system. *Appl. Microbiol. Biotechnol.* **83**, 965–77 (2009).

30. Kim, J. R. *et al.* Increasing power recovery and organic removal efficiency using extended longitudinal tubular microbial fuel cell (MFC) reactors. *Energy Environ. Sci.* **4**, 459 (2011).

31. Gálvez, A., Greenman, J. & Ieropoulos, I. Landfill leachate treatment with microbial fuel cells; scale-up through plurality. *Bioresour. Technol.* **100**, 5085–91 (2009).

32. Fangzhou, D., Zhenglong, L., Shaoqiang, Y., Beizhen, X. & Hong, L. Electricity generation directly using human feces wastewater for life support system. *Acta Astronaut.* **68**, 1537–1547 (2011).

33. Walter, X. A. *et al.* Scaling-up of a novel, simplified MFC stack based on a self-stratifying urine column. *Biotechnol. Biofuels* **9**, 93 (2016).

34. Gajda, I., Obata, O., Jose Salar-Garcia, M., Greenman, J. & Ieropoulos, I. A. Long-term bio-power of ceramic microbial fuel cells in individual and stacked configurations. *Bioelectrochemistry* **133**, 107459 (2020).

35. Ieropoulos, I. a *et al.* Waste to real energy: the first MFC powered mobile phone. *Phys. Chem. Chem. Phys.* **15**, 15312–6 (2013).

36. Ieropoulos, I., Greenman, J. & Melhuish, C. Improved energy output levels from

small-scale Microbial Fuel Cells. *Bioelectrochemistry* **78**, 44–50 (2010).

37. Papaharalabos, G. *et al.* Increased power output from micro porous layer (MPL) cathode microbial fuel cells (MFC). *Int. J. Hydrogen Energy* **38**, 11552–11558 (2013).

38. Ledezma, P., Stinchcombe, A., Greenman, J. & Ieropoulos, I. The first self-sustainable microbial fuel cell stack. *Phys. Chem. Chem. Phys.* **15**, 2278–81 (2013).

39. Winfield, J., Ieropoulos, I., Greenman, J. & Dennis, J. Investigating the effects of fluidic connection between microbial fuel cells. *Bioprocess Biosyst. Eng.* **34**, 477–84 (2011).

40. Zhuang, L. & Zhou, S. Substrate cross-conduction effect on the performance of serially connected microbial fuel cell stack. *Electrochem. commun.* **11**, 937–940 (2009).

41. Papaharalabos, G. *et al.* Dynamic electrical reconfiguration for improved capacitor charging in microbial fuel cell stacks. *J. Power Sources* **272**, 34–38 (2014).

42. Winfield, J., Ieropoulos, I., Greenman, J. & Dennis, J. The overshoot phenomenon as a function of internal resistance in microbial fuel cells. *Bioelectrochemistry* **81**, 22–7 (2011).

43. Ledezma, P. *et al.* Dynamic polarisation reveals differential steady-state stabilisation and capacitive-like behaviour in microbial fuel cells. *Sustain. Energy Technol. Assessments* **5**, 1–6 (2014).

44. You, J., Greenman, J., Melhuish, C. & Ieropoulos, I. Electricity generation and struvite recovery from human urine using microbial fuel cells. *J. Chem. Technol. Biotechnol.* **91**, 647–654 (2016).

45. Ieropoulos, I., Greenman, J. & Melhuish, C. Microbial fuel cells based on carbon veil electrodes: Stack configuration and scalability. *Int. J. Energy Res.* **32**, 1228–1240 (2008).

46. Ledezma, P., Greenman, J. & Ieropoulos, I. MFC-cascade stacks maximise COD reduction and avoid voltage reversal under adverse conditions. *Bioresour. Technol.* **134**, 158–65 (2013).

47. Aelterman, P., Rabaey, K., Pham, H. T., Boon, N. & Verstraete, W. Continuous electricity generation at high voltages and currents using stacked microbial fuel cells. *Environ. Sci. Technol.* **40**, 3388–3394 (2006).

48. Kim, J. R., Premier, G. C., Hawkes, F. R., Dinsdale, R. M. & Guwy, A. J. Development of a tubular microbial fuel cell (MFC) employing a membrane electrode assembly cathode. *J. Power Sources* **187**, 393–399 (2009).

49. Greenman, J., Gálvez, A., Giusti, L. & Ieropoulos, I. Electricity from landfill leachate using microbial fuel cells: Comparison with a biological aerated filter.

Enzyme Microb. Technol. **44**, 112–119 (2009).

50. Santoro, C. *et al.* Power generation and contaminant removal in single chamber microbial fuel cells (SCMFCs) treating human urine. *Int. J. Hydrogen Energy* **38**, 11543–11551 (2013).

51. Papaharalabos, G. *et al.* Autonomous Energy Harvesting and Prevention of Cell Reversal in MFC Stacks. *J. Electrochem. Soc.* **164**, H3047–H3051 (2017).

Table 1. Available electrical and hydraulic combinations in the 24 MFC stack

Fig 1. (A) Schematic of the eight hydraulic scenarios and MFC unit repositioning under the same waste stream. (B) Example of a 2unitsx12groups scenario with electrical connections in the stack, denoted by superscript suffixes for hydraulic units in cascade. (C) Lab-scale paradigm of the 24 MFC stack with three electrically connected assemblages, each containing eight MFC units in a hydraulic cascade (8unitsx3groups).

Fig.2 Performance characteristics from all possible cascade and electrical scenarios

Fig. 3 Breakdown of stack performance behaviour from electrical configuration and cascade scenarios

Fig. 4 Trends in internal resistance and COD removal depending on the electrical configuration

Fig. 5 COD removal correlation between power, current and R_{int}; $r_{power} = 0.249$ ($P = 0.220$), $r_{current} = 0.891$ ($P < 0.001$), $r_{Rint} = -0.891$ ($P < 0.001$)

Fig. 6 Heatmap with the optimal electrical and hydraulic combinations